连续脉冲 GTAW 熔池振荡频率的检测及分析

李春凯[1]，石　玗[2]，朱　明[1]，顾玉芬[2]
(1. 兰州理工大学 省部共建有色金属先进材料加工与再利用国家重点实验室，兰州　730050；
2. 兰州理工大学 有色金属合金及加工教育部重点实验室，兰州　730050)

摘　要：GTAW 熔池振荡频率与熔池体积具有直接物理对应关系，但其振荡频率检测较为困难，尤其在连续焊接时难度很大. 为此，提出了一种用于定点及连续焊接条件下熔池振荡频率特征检测的激光视觉测量方法. 对定点及连续焊接条件下熔池振荡频率从未熔透到全熔透的变化规律进行了研究，并对其进行了分析. 结果表明，定点焊时熔池从未熔透到全熔透仅出现一种转变模式：突变模式；在连续焊接时由于电弧作用于熔池中心点的位置偏移，造成熔池表面出现了非对称振荡模式，引起频率转变出现了两种模式：连续转变模式和突变模式. 以上频率特征可用于 GTAW 熔透的传感与控制.

关键词：激光视觉；熔池振荡；频率转变模式；连续焊接
中图分类号：TG 409　　**文献标识码**：A　　**doi**：10.12073/j.hjxb.20151120004

0　序　　言

焊缝熔透状态对焊缝力学性能具有决定性影响，许多重要的结构件为保证质量都对焊缝熔透状态提出了较高的要求. 因此，实现熔透的实时控制对提高生产效率、保证焊接质量具有重要意义.

由于熔池体积与熔池振荡频率之间有较为直接的物理对应关系，若能可靠检测熔池特征振荡频率则可取得较好的控制效果. 文献[1－3]利用脉冲电流激振熔池产生振荡并采集电弧电压信号，通过傅里叶变换得到了熔池特征振荡频率. 文献[4－5]提出了一种熔池谐振法，通过改变附加正弦波电流频率获得不同频率下的熔池尺寸. 由于熔池表面振荡幅度很小，一般为 0.2～0.4 mm[6]，且在焊枪连续行走时电弧作用中心点发生偏移，熔池激振困难，反映到弧压、弧光信号上信噪比低. 以上方法目前只适用于定点或步进焊，限制了其在生产中的应用.

针对传统弧光、弧压法信噪比低，无法用于连续焊接的缺点，运用熔池表面受激产生振荡及熔池表面的类镜面特性原理，提出了一种激光视觉测量法，用于定点及连续焊接熔池振荡频率检测；对定点及连续焊接时熔池从未熔透到全熔透的频率变化模式进行了试验研究，得到了不同焊接条件下熔池振荡频率变化模式，并对其进行了分析.

收稿日期：2015－11－20
基金项目：国家自然科学基金资助项目(51305189)；兰州理工大学红柳杰出人才培养计划资助项目(J201201)；省部共建有色金属先进加工与再利用国家重点实验室开放基金资助项目(SKLAB02015008)；兰州理工大学优秀学生出国学习交流基金资助项目

1　试验方法

利用熔池表面的镜面特性和反射激光条纹对熔池振荡行为的放大作用，提出了激光视觉熔池振荡检测法，原理如图 1a 所示. 将激光条纹投射于熔池

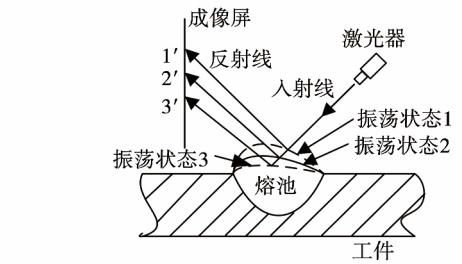

(a) 激光视觉原理

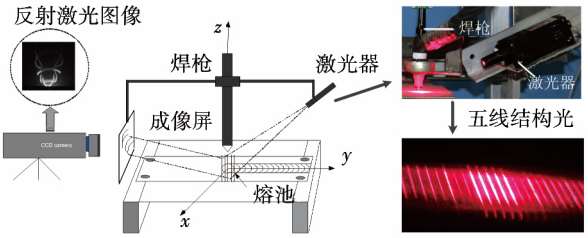

(b) 试验系统简图

图 1　激光视觉原理及试验系统
Fig. 1　Principle of laser vision and sensing system

表面，当熔池表面发生振荡时，振幅很小但引起的激光反射角度变化很大，在成像屏上成像后相当于对振荡行为进行了光学放大. 图 1b 为搭建试验平台结构简图. 由于熔透时的振荡频率一般低于 100 Hz[3]，因此将摄像机采样频率定为 800 Hz.

图 2 为采集的峰值电流 $I_p = 144$ A，基值电流 $I_b = 40$ A，占空比 $\sigma = 40\%$，脉冲频率 $f = 3.5$ Hz，焊接速度为 $v = 1.0$ mm/s 时采集的典型激光条纹. 脉冲峰值阶段熔池表面受到较强等离子流力冲击，表面发生压缩变形. 基值阶段由于等离子流力突然变小，熔池表面将在重力、表面张力的合力提供回复力作用下发生振荡，进而引起激光条纹发生周期性“收缩”与“舒张”. 观察图 2 可以看出激光条纹变化表现出了明显的周期性，这种“收缩膨胀”使整个图像亮度值发生周期性变化，文献[6-7]提出了亮度值法计算标定窗口内的像素值，将窗口内亮度值大小作为熔池振荡时域信号并对其进行快速傅里叶变换(FFT)得到熔池振荡频率.

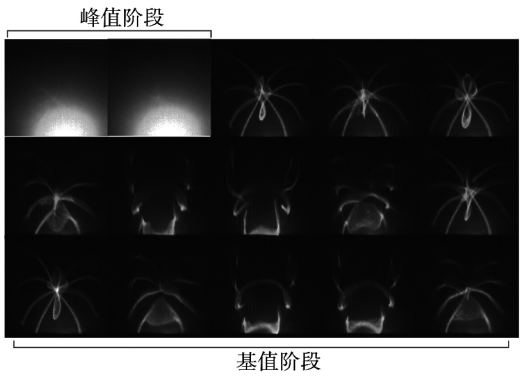

图 2 典型激光条纹图像

Fig. 2 Typical laser reflected pattern

为了研究定点及连续焊接熔池振荡频率变化规律，在 4 mm 不锈钢板上进行了 3 组工艺试验，试验参数如表 1 所示. 其中参数 1 为定点焊试验，通过改变电弧作用时间来获得不同熔深、熔透的熔池. 参数 2 和参数 3 为连续焊接试验，通过改变焊接速度来获得不同熔透、熔深的熔池.

表 1 焊接工艺参数

Table 1 Welding parameters

组号	峰值电流 I_p/A	基值电流 I_b/A	占空比 σ(%)	平均电流 I/A	脉冲频率 f/Hz	焊接速度 v/(mm·s^{-1})
1	160	50	30	83	3.5	0
2	144	70	44	102.66	3.5	2.1～1.0
3	220	60	54	146.4	3.5	3.1～2.1

2 试验结果

2.1 定点焊熔池振荡频率转变规律

采用表 1 中参数 1，通过不同电弧作用时间获取不同熔深、熔透的激光反射条纹并采用亮度值法得到了熔池固有振荡频率. 图 3 为电弧作用时间为 4 s 时未熔透时的熔池振荡的时域及频域信号. 可以看出，采用亮度值法得到的熔池振荡时域信号变化范围大、周期性强，对其进行频谱变换后，发现熔池振荡特征频率明显、性噪比高.

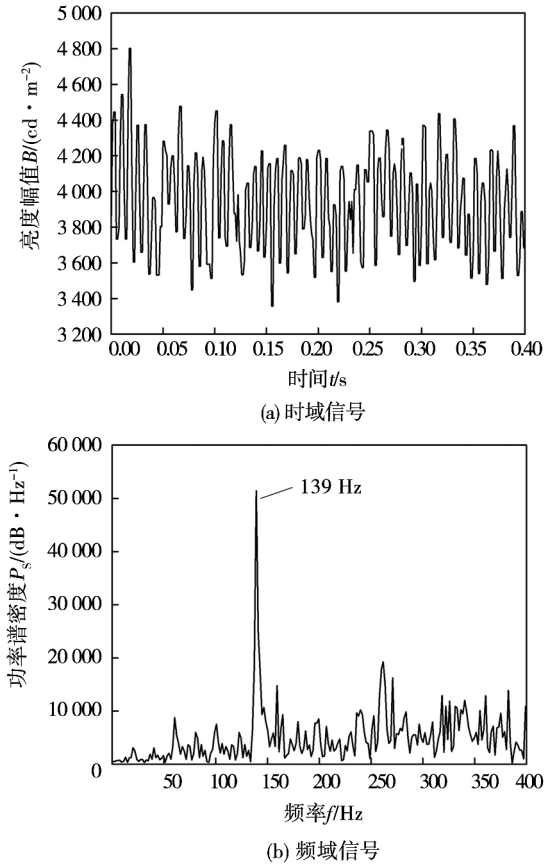

图 3 定点焊未熔透振荡信号

Fig. 3 Signals of partial penetration oscillation

图 4 为振荡频率从未熔透到全熔透的变化，可以发现，熔池在未熔透时振荡频率较高，一般在 100 Hz 以上，且随着正面熔宽的增大而增大；当熔池到达全熔透状态时，频率信号发生了突变，直接降到 70 Hz 以下；通过上述分析可以得出定点焊时熔池振荡频率变化规律为突变模式，即从未熔透到全熔透时频率出现了突变.

2.2 连续焊熔池频率转变规律

采用表 1 中参数 2 和参数 3，通过改变焊接速度采集了不同熔深、熔透的反射条纹，并获取了熔池振

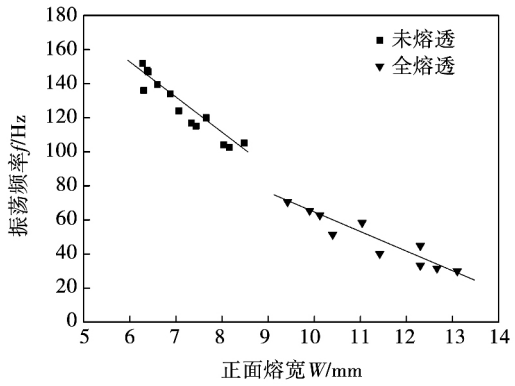

图 4　定点焊频率变化

Fig. 4　Frequency change in stationary condition

荡频率. 图 5为焊接速度 1.2 mm/s 时全熔透时的时域及频域信号. 可以看出熔池在全熔透状态下时域信号周期变长且出现了明显衰减,通过傅里叶变换后得到的熔池特征频率明显、信噪比高.

图 6a,b 分别为采用参数 2,参数 3 得到的频率变化. 采用参数 2 时熔池从未熔透到全熔透出现了频率的突变,未熔透时振荡频率一般在 100 Hz 以上,全熔透时频率低于 70 Hz. 采用参数 3 时,熔池振荡频率低于 85 Hz,从未熔透到全熔透没有频率突变, 50 ~ 60 Hz 之间出现了频率的重叠. 因此,连续焊接时振荡频率变化存在两种模式: 突变和连续转变模式.

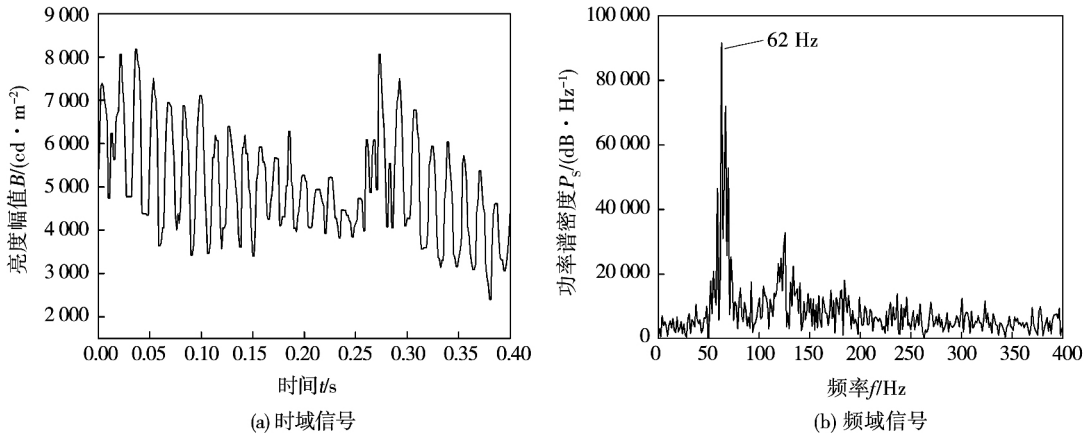

(a) 时域信号　　(b) 频域信号

图 5　连续焊全熔透振荡信号

Fig. 5　Signals of full penetration oscillation

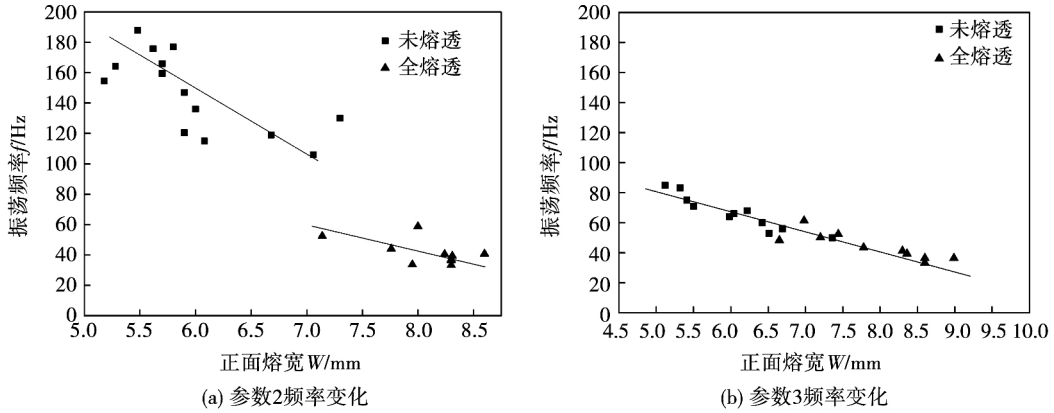

(a) 参数2频率变化　　(b) 参数3频率变化

图 6　连续焊频率变化

Fig. 6　Frequency change in continuous condition

3　分析及讨论

3.1　未熔透时熔池振荡频率变化分析

通过分析定点及连续焊接时未熔透振荡频率变化规律可知,未熔透时存在两种频率变化模式: 较高模式和较低模式. 在较高模式下熔池振荡频率高于 100 Hz; 较低模式只出现在连续焊接时. 从熔池表面振荡状态对两种模式进行分析.

在定点焊时电弧作用点与熔池中心一致,在基值阶段脉冲电弧力减小时将会发生如图 7a 所示的对称振荡. 在连续焊接时,熔池被拖长,电弧作用于

熔池表面位置从中心偏移到了熔池前部，根据焊接参数不同将会出现两种振荡模式. 在参数 2 下，焊接速度较低，电弧作用力相对熔池中心点的偏移量较小，同时峰值电流较小、脉冲电弧力过小，不足以将熔池中液态金属推到熔池后方，其表面振荡仍然以定点焊时的对称振荡模式进行振荡，振荡模式示意图如图 7b 所示; 而在参数 3 下，焊接速度较大，引起电弧作用点相对熔池中心点的偏移量增加，使得熔池前部与后部出现不对称，同时峰值电流增大使得脉冲电弧力增加，将熔池中大部分液态金属推到了电弧后方，基值阶段电弧力减小时，熔池表面将出现如图 7c 所示的非对称“晃动”振荡模式. 文献 [3] 采用自由表面波理论对对称振荡和“晃动”模式进行了建模，结果表明对称振荡模式下的振荡频率高于“晃动”模式，这与试验结果一致.

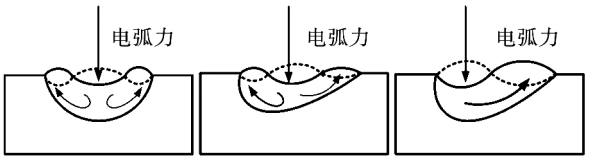

(a) 定点振荡模式 (b) 连续振荡模式1 (c) 连续振荡模式2

图 7 未熔透时表面振荡模式

Fig. 7 Surface oscillation mode in partial penetration

3.2 全熔透时熔池振荡频率变化分析

通过分析定点及连续焊接时全熔透的振荡频率变化规律可得，全熔透时振荡频率很低，低于 70 Hz，且随着正面熔宽的增大、熔池体积的增大而逐渐减小. 从熔池表面波动及内部流动的角度对其进行分析.

在全熔透时熔池中的液态金属不再受到背面固态金属的支撑，主要靠熔池正反面液态金属的表面张力来支撑. 在定点焊时由于电弧力对称，在基值阶段熔池表面将发生类似于以“二维薄膜”的对称振荡，如图 8a 所示; 在连续焊接时，电弧作用相对于熔池非对称，但由于熔池背面无支撑，在峰值电流过大时并不会引起类似于未熔透时较强的电弧力而将熔池金属推向后方，在基值阶段脉冲电弧力减小时，熔池表面将主要以垂直振荡为主，可近似看成定点焊时的对称振荡[3]. 因此，在全熔透状态下定点或连续的振荡频率并没有出现较大的差异.

在连续焊接时由于“晃动”模式的出现，使得熔池振荡频率从未熔透到全熔透出现了连续转变模式，而连续转变模式不利于后续通过频率信号实现熔透控制，因此需要对对称振荡模式和“晃动”模式影响因素进行进一步研究.

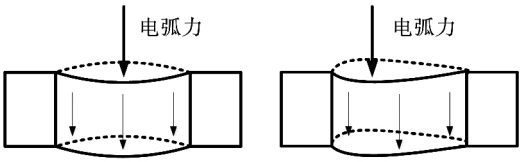

(a) 定点全熔透振荡模式 (b) 连续全熔透振荡模式

图 8 全熔透时表面振荡模式

Fig. 8 Surface oscillation mode in full penetration

4 结 论

(1) 提出了一种基于激光视觉的检测方法，并实现了定点及连续熔池振荡频率的检测.

(2) 对定点及连续焊接条件下熔池从未熔透到全熔透频率变化规律进行了研究. 定点焊时熔池从未熔透到全熔透出现一种转变模式: 突变模式; 在连续焊接时两种模式: 突变和连续转变模式，且焊接工艺参数对振荡模式有重要影响.

参考文献:

[1] Renwick R J, Richardson R W. Experimental investigation of GTA weld pool oscillations [J]. Welding Journal, 1983, 62(2): 29 – 35.

[2] Xiao Y H, Den Ouden G. A Study of GTA weld pool oscillation [J]. Welding Journal, 1990, 69(8): 289 – 293.

[3] Xiao Y H, Den Ouden G. Weld pool oscillation during welding of mild steel [J]. Welding Journal, 1993, 72(8): 184 – 192.

[4] 杨春利，何景山，王其隆，等. TIG 焊变频电流下熔池谐振检测与研究 [J]. 焊接学报, 2000, 21(2): 6 – 9.
Yang Chunli, He Jingshan, Wang Qilong, *et al*. Acquisition of molten pool resonance in TIG welding with fluctuant frequency Current [J]. Transactions of the China Welding Institution, 2000, 21(2): 6 – 9.

[5] 杨春利，张九海，王其隆. TIG 焊熔池外激谐振与熔透的关系 [J]. 焊接学报, 1990, 11(4): 193 – 198.
Yang Chunli, Zhang Jiuhai, Wang Qilong. Relationship between the weld pool resonance and the weld full penetration in TIG welding [J]. Transactions of the China Welding Institution, 1990, 11(4): 193 – 198.

[6] 石 玗，李春凯，顾玉芬，等. 脉冲钨极气体保护焊熔池振荡频率激光视觉测量 [J]. 上海交通大学学报, 2016, 50(12): 1910 – 1914.
Shi Yu, Li Chunkai, Gu Yufen, *et al*. Measurement of weld pool oscillation for pulsed GTAW based on laser vision [J]. Journal of Shanghai Jiaotong University, 2016, 50(12): 1910 – 1914.

[7] Shi Y, Zhang G, Ma X J, *et al*. Laser-vision-based measurement and analysis of weld pool oscillation frequency in GTAW-P [J]. Welding Journal, 2015, 94(3): 176 – 184.

[8] Maruo H, Hirata Y. Natural frequency and oscillation mode of weld pool [J]. Japan Welding Society, 1993, 11(1): 50 – 54.

作者简介: 李春凯，男，1990 年出生，博士研究生. 主要研究方向为焊接过程控制及自动化. 发表论文 3 篇. Email: 15339316249@163.com

通讯作者: 石 玗，男，教授，博士研究生导师. Email: shiyu@lut.cn

Key words: SiO_2 ceramic; TC4 alloy; active filler metal; brazing; interfacial microstructure

Detection and analysis of weld pool oscillation frequency for continuous P-GTAW LI Chunkai[1], SHI Yu[2], ZHU Ming[1], GU Yufen[2] (1. State Key Laboratory of Advanced Processing and Recyling of Nonterrous Metals, Lanzhou University of Technology, Lanzhou 730050, China; 2. Key Laboratory of Nofferrous Metal Alloys of Ministry of Education, Lanzhou University of Technology, Lanzhou 730050, China). pp 43 - 46

Abstract: There exists a direct relationship between the weld pool oscillation frequency and volume of weld pool. But the detection of oscillation frequency in continuous condition is difficult. A new laser-vision method was proposed for detecting the weld pool oscillation frequency under the condition of stationary and continuous welding. In order to study the rule of weld pool oscillation frequency from partial penetration to full penetration, several experiments with stationary and continuous condition were conducted and the change mode of frequency was analyzed. The results showed that from partial penetration to full penetration, there was a mutation mode in stationary condition. In continuous condition, the weld pool was elongated and the arc had an asymmetrical position with respect to weld pool center, which resulted in two change mode, mutation mode and continuous mode. This characteristic of frequency can be used in sense and control of weld pool penetration of GTAW.

Key words: laser-vision; weld pool oscillation; change mode of oscillation frequency; continuous welding

Single welding torch coupled arc AA-TIG welding ZHANG Jianxiao[1,2], FAN Ding[1], HUANG Yong[1] (1. State key Laboratory of Advanced Processing and Recycling of Nonferrous Metals, Lanzhou University of Technology, Lanzhou 730050, China; 2. Lanzhou Lanshi Heavy Equipment Co. Ltd., Lanzhou 730314, China). pp 47 - 50

Abstract: By using the improved welding torch, coupled arc AA-TIG welding experiments were carried out with SUS304 plate as the base metal. The differences of arc morphology and weld shape between AA-TIG welding and traditional TIG was compared. Meanwhile the effects of major parameters to AA-TIG weld bead as well as the weld mechanical properties were investigated. The results showed that the welding parameters including oxygen flowrate, electrode spacing and arc length had significant influences on the weld penetration of coupled arc AA-TIG welding. Under the same total current, the welding bead of coupling AA-TIG was narrower and deeper when comparing with conventional TIG welding. The weld presented better mechanical properties. For 12 mm thickness SUS304 stainless steel plate, the weld penetration of one pass exceeded 11mm, the weld depth/width ratio reached 1.3. The welding productivity was improved dramatically.

Key words: AA-TIG welding; coupled arc; welding torch; weld shape; weld property

Laser-TIG arc hybrid welding technology of 6005A aluminum alloy with filler wire YANG Dawei[1], CHEN Shuhai[1], HUANG Jihua[1], FENG Xiaosong[2], LU Hao[3] (1. School of Materials Science and Technology, University of Science and Technology Beijing, Beijing 100083, China; 2. Shanghai Aerospace Eeuipments Manufacturer, Shanghai 200245, China; 3. CRC Qingdao Sifang Co., LTD, Qingdao 266111, China). pp 51 - 54

Abstract: 6005A aluminum alloy which is used for high-speed vehicle was welded by a new technology of laser-TIG arc hybrid welding with filler wire. According to the research of hybrid welding process, microstructure of the joints, mechanical properties, fracture morphology and welding hot cracking, welding process was relatively stable and welding appearance were perfect when laser power was in the range of 2 000 W to 3 000 W, TIG current was 150-195 A, welding speed was 0.4 ~ 0.8 m/min. Welding zone was composed of columnar grains in the edge of welding seam and equiaxed grains in the center of welding seam. The average tensile strength of joint was about 193.39 MPa and joint tensile strength increased with the increase of penetration ratio. In addition, the maximum tensile strength was about 205 MPa—70% of the strength of base metal when penetration ratio was 0.7.

Key words: 6005A aluminum alloy; laser-TIG hybrid welding; microstructure; mechanical properties

Numerical analysis model of temperature field in swing-arc narrow gap GMAW XU Guoxiang, PAN Haichao, WANG Jiayou (Key Laboratory of Advanced Welding Technology of Jiangsu Province, Jiangsu University of Science and Technology, Zhenjiang 212003, China). pp 55 - 60

Abstract: Based on macro thermal transfer theory and geometric feature of weld cross section, the heat source model for swing-arc narrow gap GMAW is developed after considering the influence of arc swing, geometric feature of welded joint and weld surface shape on arc heat flux distribution. By using ANSYS software, the transient temperature profile and thermal cycle curve in swing arc narrow gap GMAW are calculated and their distribution features are analyzed. The results show that the established heat source model can reflect the moving path of swing arc and its thermal action feature and the calculated geometry and size of weld cross section agree well with the experimental data, validating the accuracy of the developed model. At 300A welding current and 2 Hz swing frequency, the weld pool changes limitedly.

Key words: swing arc narrow gap welding; heat source model; temperature field; numerical simulation

Numerical simulation of shunting in resistance spot welding for dissimilar unequal-thickness aluminum alloys ZHANG Yu[1], BI Jing[2], LUO Zhen[1,3], LI Yang[1] (1. School of Materials Science and Engineering, Tianjin University, Tianjin 300072, China; 2. Tianjin Long March Launch Vehicle Manufacturing Co. Ltd., Tianjin 300462, China; 3. State Key Laboratory of Advanced Welding and Joining, Harbin Institute of Technology, Harbin 150001, China). pp 61 - 65

Abstract: The model of shunting in resistance spot welding for dissimilar unequal-thickness aluminum alloys 2219/5052 is established by using ANSYS software in the paper. The effect of different weld spacing between two welds on shunting and nugget diameter is researched. The mechanism of shunting in resistance spot welding is analyzed, and a processing method for improving shunting is proposed. The calculated results show that the smaller the weld spacing is, the larger the shunting is. The nugget is not formed when the weld spacing is 12 mm. Shunting can be diminished and improved by increasing current. Experiments verify that the nugget diameter of numerical calculation a-